

## Crack detection in subway tunnels based on multi-feature analysis

FAN Weiwei, WANG Xiaopeng\*, ZHU Shengyang

School of Electronic & Information Engineering, Lanzhou Jiaotong University, Lanzhou 730070, China

\*Corresponding author: WANG Xiaopeng (wangxiaopeng@mail.lzjtu.cn)

Received: September 19, 2023

Revised: November 27, 2023

Accepted: December 14, 2023

**Abstract:** In the process of crack detection in subway tunnels, it is difficult to detect tunnel cracks due to the complexity of tunnel environments and the limitation of light conditions. To this effect, a tunnel crack detection method based on multi-feature analysis was proposed. Firstly, the quality of the tunnel crack image was improved by the preprocessing algorithm combining Retinex smoothing and piecewise linear stretching, and then the image was preliminarily segmented by Otsu threshold algorithm for block processing. Secondly, the area and rectangularity of connected domain in the image were analyzed, the linear structural features in the image were extracted by probabilistic Hough transform, and the pseudo crack interference was filtered out by image skeleton feature extraction algorithm. Finally, real crack detection was realized, and the detection rate of traditional crack image and tunnel crack image reached 92% and 86%, respectively. It is experimentally verified that the proposed method is practical and effective.

**Key words:** subway tunnel; crack detection; multi-feature analysis; connected domain

### 0 Introduction

As one of the most common and serious defects on the surface of subway tunnels, cracks may cause structural collapse and seepage if they are not treated in time, thus affecting the safe operation of subways. Therefore, the periodic detection of tunnel cracks becomes particularly important. Traditional tunnel crack detection methods are mainly based on manual detection, which is difficult to accurately detect the cracking degree and specific location of cracks<sup>[1]</sup>. With the continuous progress of machine vision technology and digital image processing technology, the crack detection methods based on digital image processing technology have become the main research direction because of their high timeliness, convenience and intuitiveness<sup>[2]</sup>.

At present, many achievements have been made in crack detection based on digital image processing technology. Wang et al.<sup>[3]</sup> designed a tunnel crack detection system, and the proposed image recognition algorithm can effectively detect ordinary crack images. Tang et al.<sup>[4]</sup> adopted a method combining threshold and edge for image segmentation to avoid low accuracy of traditional Otsu segmentation algorithm. Li et al.<sup>[5]</sup> proposed a crack detection method based on minimum path search, which has strong anti-spot noise ability. Wang et al.<sup>[6]</sup> proposed a

crack extraction algorithm based on seed point growth, which can effectively avoid repeated marking of cracks. Wang et al.<sup>[7]</sup> proposed a gradient inter-class threshold segmentation algorithm based on Prewitt operator and Otsu threshold algorithm by delineating the features of each connected domain for crack extraction. Xu et al.<sup>[8]</sup> used *K*-means clustering algorithm to analyze the area of connected domain, the minimum length-width ratio of the connected domain bounding box and the furthest distance in connected domain in crack image. Oliveira et al.<sup>[9]</sup> designed two classifiers to detect cracks and judge the type of cracks, respectively. Medina et al.<sup>[10]</sup> accurately calculated crack pixels based on crack edge detection algorithm. Salari et al.<sup>[11]</sup> used support vector machine (SVM) to separate cracks in the image from the background, and then used thresholds to extract cracks.

Compared with ordinary pavement crack images, subway tunnel crack images generally have uneven gray distribution, large illumination changes, poor spatial connectivity, complex texture structures and therefore they are easily interfered by factors such as pipes, seams, scratches, etc. To solve these problems, we proposed a method based on multi-feature analysis for the crack detection of subway tunnel surface images, which used Retinex smoothing and piecewise linear stretching for image preprocessing, Otsu threshold

algorithm for block segmentation, probabilistic Hough transform for linear structural feature extraction and image skeleton feature extraction algorithm for filtering out pseudo crack interference.

## 1 Detection process of cracks of subway tunnel

A new preprocessing algorithm was first proposed to deal with uneven illumination and low contrast in tunnel crack images. Furthermore, a new crack detection method based on multi-feature analysis of connected domain features, linear structural features and crack texture skeleton features was also presented. The detection process is shown in Fig.1.

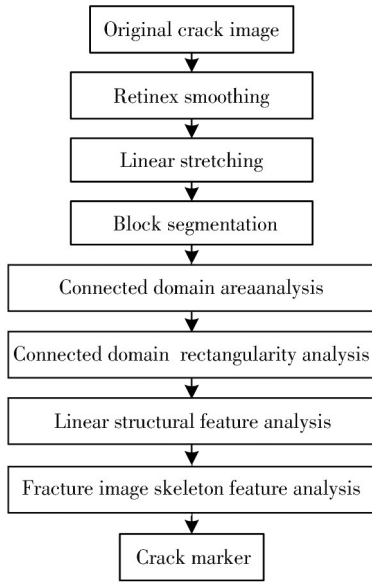


Fig. 1 Detection process of cracks of subway tunnel

## 2 Image preprocessing and block segmentation

### 2.1 Image preprocessing

Since there are generally no strong light sources in subway tunnels, array light sources are often required for auxiliary illumination during image acquisition, which may result in the uneven gray distribution of collected images and less prominent image details. Therefore, it is difficult to detect defects directly from the image background. The traditional methods usually use histogram equalization and linear stretching to deal with them, but there are certain drawbacks. In our work, Retinex smoothing and linear stretching<sup>[12]</sup> were combined to inhibit the influence of these factors.

Firstly, Retinex smoothing algorithm was utilized to uniformly process the image gray. It divides the image

$S(x,y)$  into two parts: illumination component  $L(x,y)$  and reflection component  $R(x,y)$ . For a specific image, the relationship is expressed as

$$S(x,y) = R(x,y)L(x,y). \quad (1)$$

In Retinex smoothing algorithm, illumination component is to compensate for reflection component, so that the image is enhanced. The specific steps include: 1) Construct Gaussian surround function; 2) Use the constructed Gaussian function to filter three channels of color images; and 3) Subtract the incident component from the original image in logarithmic domain and then obtain the reflection component as output image. Its essence is to remove the smooth part of the original image and highlight the rapid change part of the original image. The gray level of the crack edge is a part of the image that changes rapidly, so it can be used to enhance the image and highlight the edge of the image. The calculation process is expressed as

$$R_i(x,y) = \log \left[ \frac{S_i(x,y)}{L_i(x,y)} \right] = \log S_i(x,y) - \log [F(x,y) * S_i(x,y)], \quad (2)$$

where  $i$  represents the color channel;  $S_i(x,y)$  represents the low-light image input by the first  $i$  color channel;  $R_i(x,y)$  represents the output of the first channel after Retinex processing;  $*$  is the convolution operator; and  $F(x,y)$  represents Gaussian surround function, which is expressed as

$$F(x,y) = \lambda e^{-(x^2+y^2)/c^2}, \quad (3)$$

where  $c$  is the proportional constant, and  $\lambda$  is the normalized coefficient. Since the integral of  $F(x,y)$  is always equal to 1, the value of  $F(x,y)$  can be calculated.

Secondly, the piecewise linear stretching calculation of the image was worked out. According to the distribution range of the gray level in gray histogram of the original image, the gray interval of interest was linearly stretched, and other intervals were compressed to improve the contrast of the image. The specific process is expressed as

$$f_1(x,y) = a * f(x,y) + b, \quad (4)$$

where  $f(x,y)$  is the original image;  $f_1(x,y)$  is the linear stretching image;  $a$  is the slope; and  $b$  is the intercept.

As shown in Fig.2, histogram equalization adjusts the gray distribution of the image globally, but when it is applied to an image with uneven illumination, it will make the unevenness more obvious. Linear stretching linearly transforms the gray value of the entire image, so that the gray space of the original image becomes larger,

and the difference between the feature area and the background increases, but it fails to play the role of uniform brightness, which is not conducive to the subsequent detection of cracks. The method based on Retinex uniform light and piecewise linear stretching effectively balance the illumination, protects image details, improves the contrast of cracked images, and lays a foundation for accurate segmentation of images.

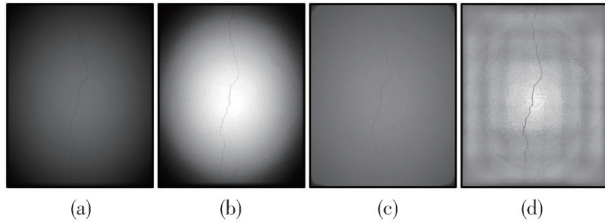


**Fig. 2 Image preprocessing comparison. (a) Original image; (b) Histogram equalization; (c) Linear stretching; (d) Retinex combined with linear stretching**

## 2.2 Block segmentation

For the background interference of subway tunnel images, there are still many impurities after traditional Otsu segmentation, which is not conducive to subsequent crack detection. After the image is divided into blocks and segmented by Otsu algorithm, the binary image with less impurities and complete cracks can be obtained.

Let  $f(x,y)$  be the gray value at point  $(x,y)$  and  $g(x,y)$  be the segmented image, the basic principle of threshold segmentation is expressed as

$$g(x,y) = \begin{cases} 1, & f(x,y) > T, \\ 0, & f(x,y) \leq T, \end{cases} \quad (5)$$

where  $T$  is the threshold. The background of the crack image on the tunnel surface is complex and contains a lot of interference information, of which cracks only account for a small part, and the grayscale histogram of the image does not have obvious bimodal characteristics<sup>[13]</sup>. Therefore, it is very important to calculate the appropriate threshold for the segmentation results. In this study, the method of block segmentation was used to perform preliminary segmentation of the images containing cracks. Firstly, the gray image of an image was divided into multiple image blocks. To avoid more blocks, the size of each image block was set to be  $50 \times 50$  pixels. Secondly, the Otsu threshold algorithm was used to calculate the threshold of each image block, and the image blocks containing only background and cracks were distinguished by the calculated threshold and interclass variance. Thirdly, each image block was segmented by Otsu method. Finally, the segmentation

results of each image block were spliced according to the original position to obtain the final segmentation results.

## 3 Feature analysis and crack identification

After the tunnel crack image is processed by the above block segmentation, the main components include the real crack texture component, the noise component, the linear structure interference component and the pseudo crack component.

According to the experience of crack detection in artificial tunnels, it is found that there are some different characteristics between cracked structures and non-cracked structures. The cracks are narrow and elongated targets with a certain orientation and poor cohesion. The lengths of cracks are generally larger than that of non-crack structures, which have a certain continuity in space, and the pixels in the same crack area are connected. The widths of the cracks are small, the directions of the cracks are single, and the refined binary texture skeleton image is not much different from the original image, while the pseudo crack has a large width, a complex direction, and a large difference between the binary texture skeleton and the original image.

Therefore, the interference of non-cracked structures can be removed gradually by analyzing the characteristics of the components. The noise component mainly include isolated point noise and block noise, which can be extracted by the connected domain area and rectangularity, respectively. The pipeline and joint show linear characteristics after segmentation, so we adopted probabilistic Hough transform to analyze the linear structure characteristics of tunnel surface. The pseudo crack component mainly includes texture features such as scratches and stains. In this study, real cracks and pseudo crack textures were identified according to the difference of their feature.

### 3.1 Area of connected domain

In the tunnel surface image, there are many isolated point noises, which occupy a small number of pixels. Filtering in the connected domain will not change the details of the image, while the traditional median filter denoising depends on the size of filter window, which has a great impact on the quality of output image. If the window is too small, the denoising effect will be poor; if the window is too large, many image details will be lost and the image will be blurred. In this study, filtering was performed by analyzing the zero-order moment  $N_k$  of the

connected domain  $C_k(x, y)$ . The filter process is expressed as

$$N_k = \sum_x \sum_y [1 - P_k(x, y)], \quad (6)$$

$$i_a(x, y) = \{C_k(x, y) | N_k < T_n, k = 1, 2, \dots, N_n\}, \quad (7)$$

where  $P_k(x, y)$  is the gray value at point  $(x, y)$  of each connected region  $C_k(x, y)$ ;  $i_a(x, y)$  represents the isolated point noise component;  $N_n$  is the number of isolated point noise connected domains in the image;  $T_n$  is zero-order moment threshold. The noise points in the connected domain with the number of pixels less than the threshold are removed.

### 3.2 Rectangularity of connected domain

Compared with isolated point noise, block noise occupies a large number of pixels and a certain area, and has obvious aggregation, which is different from the long and narrow crack structure. Therefore, block noise can be filtered by calculating the rectangularity of the connected domain to analyze its cohesion. The rectangularity of connected domain can be expressed by

$$R_k = \frac{\sum_x \sum_y [1 - P_k(x, y)]}{S_M} = \frac{N_k}{S_M}, \quad (8)$$

$$i_b(x, y) = \{B_k(x, y) | R_k > T_r, k = 1, 2, \dots, N_R\}, \quad (9)$$

where  $R_k$  is the ratio of the connected domain area to the external rectangular area;  $i_b(x, y)$  stands for speckle noise;  $N_R$  is the number of speckle noise regions  $B_k(x, y)$  in  $i_b(x, y)$ ;  $T_r$  is the rectangularity threshold. The connected domain with the rectangle degree greater than threshold  $T_r$  is considered as block noise.

### 3.3 Linear structure features

Hough transform is a method for linear detection in the parameter space. A point in the image coordinate space is mapped to the parameter space as a straight line. The probabilistic Hough transform is a deformation of the standard Hough transform. It only randomly selects a pixel from the point set for analysis. To a certain extent, this method reduces the computing time, and thus is widely used in the detection of graphics such as lines and circles. Since cracks also exhibit linear characteristics in a small range<sup>[14]</sup>, setting a threshold for the length of detected straight line can effectively prevent cracks from being removed. The specific steps are as follows.

1) Randomly select a feature point from the point set. If the point has been calibrated as a point in a straight

line, continue to randomly select other feature points until all features are selected.

2) Perform Hough transform on the selected feature points, and then perform accumulation and calculation.

3) Select the point with the largest value in the Hough space. If the point is greater than the threshold, go to step 4, otherwise go back to step 1.

4) Take the maximum value obtained by the Hough transform as starting point and move along the direction of the line, the endpoint of the line can be found.

5) Calculate the length of the straight line. If it is greater than a certain threshold, it is considered as a straight line, and return to step 1.

### 3.4 Image skeleton feature extraction in connected domain

According to the skeleton characteristics of the crack image, the ratio of the skeleton map of the selected pixel area to the binary map of the removed linear structure was used to identify the real crack image<sup>[15]</sup>. Firstly, the skeleton map of the connected domain image was extracted. In the binary image with the linear structure removed, the target pixel point and the boundary pixel point were recorded as 1, the background pixel point was recorded as 0, and each area in the image was more than a single pixel thickness. Then, the image was iteratively transformed point by point according to the values of adjacent points in the connected domain. Assuming that the center pixel is  $P_1$ , and the points of its 8 connected neighbors are  $P_2, P_3, \dots, P_9$ , respectively, as shown in Fig. 3, the iterative process of image refinement algorithm for boundary points includes two steps:

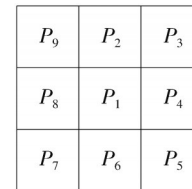


**Fig. 3 Schematic diagram of refinement algorithm**

1) Loop through all foreground pixels and mark the boundary points that meet the following conditions as

$$\begin{cases} 2 \leq M(P_1) \leq 6, \\ N(P_1) = 1, \\ P_2 P_4 P_6 = 0, \\ P_4 P_6 P_8 = 0, \end{cases} \quad (10)$$

where  $M(P_1)$  is the number of foreground pixels in the eight-connected neighborhood of  $P_1$ ;  $N(P_1)$  refers to

the number of occurrences between adjacent pixels in the order of  $P_2, P_3, \dots, P_9, P_2$ . When all boundary points have been verified, all marked points are deleted.

2) Similar to step 1, mark boundary points that meet the following conditions as

$$\begin{cases} 2 \leq M(P_1) \leq 6, \\ N(P_1) = 1, \\ P_2 P_4 P_8 = 0, \\ P_2 P_6 P_8 = 0. \end{cases} \quad (11)$$

In Eq. (11), after the inspection of all boundary points is completed, all marked points are deleted. Eqs. (10) and (11) are used for iterative operation, and the candidate crack connected region is iteratively calculated for many times until no pixel satisfies the condition to be marked. At the end of the algorithm, the skeleton map of the crack region is formed.

The schematic diagram of crack texture and pseudo crack texture skeleton is shown in Fig. 4. The image skeleton can clearly describe the geometric structure and topological properties, the crack skeleton is composed of some points that can fully describe the fracture morphology characteristics of the curve. The number of crack pixels in the segmented binary image is not much different from that in the skeleton image. Since the texture features of pseudo cracks are complex and the extracted skeleton morphology changes greatly, the skeleton texture features were used to identify cracks.

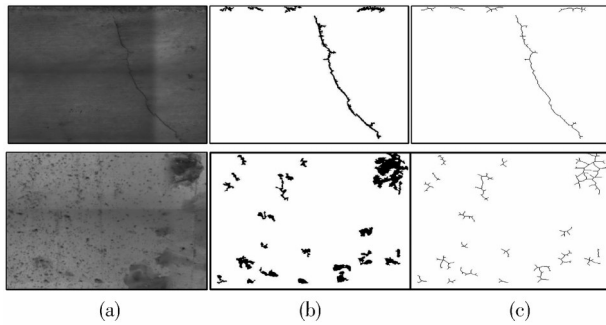


**Fig. 4 Skeleton diagram of crack texture and pseudo crack texture. (a) Original crack images; (b) Binary images; (c) Skeleton images**

Firstly, calculate the number of pixels  $n_k$  in the crack area  $z_k(x, y)$  of the binary image to be identified. Then, calculate the number of pixels  $m_k$  in the target texture of the skeleton image  $\delta_k(x, y)$  corresponding to the area. Finally, calculate the ratio  $t_k$  between the number of target pixels  $n_k$  in the binary image and the number of target pixels  $m_k$  in the skeleton image. The calculation process is shown as

$$m_k = \sum_x \sum_y [1 - \delta_k(x, y)], \quad (12)$$

$$t_k = n_k / m_k. \quad (13)$$

## 4 Experiment and analysis

To verify the applicability and effectiveness of the proposed method, 100 crack images captured in engineering projects were simulated and tested, including 50 ordinary crack images and 50 tunnel crack images, and Matlab was used for programming simulation.

### 4.1 Step-by-step verification of subway tunnel crack image detection

The step-by-step detection results are shown in Fig.5.

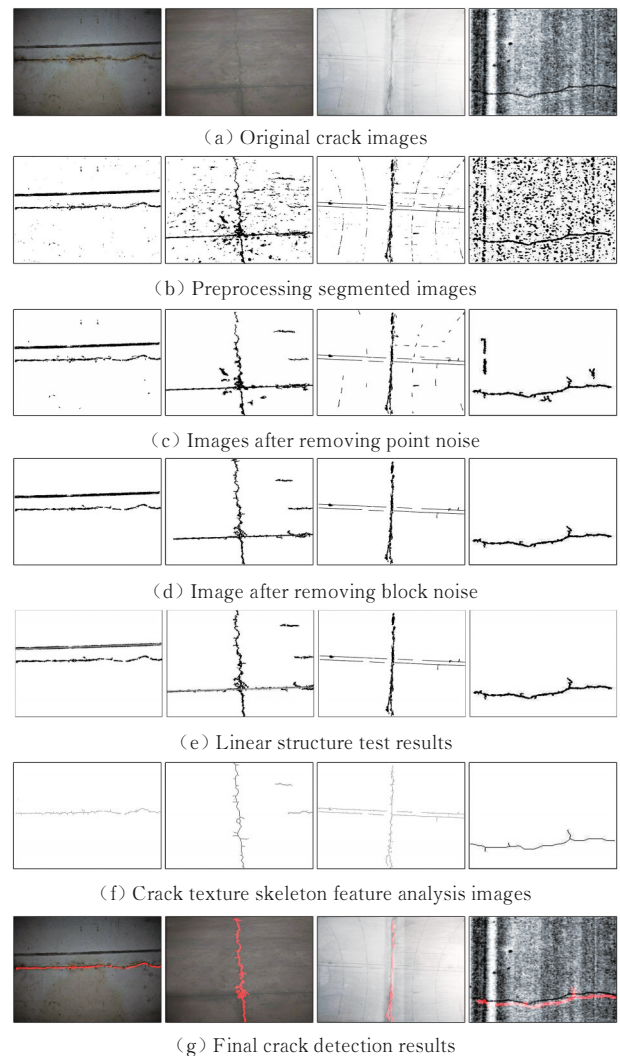


**Fig. 5 Typical crack image detection experiment**

Fig. 5(a) shows four original images with sizes of  $1440 \times 1080$  pixels,  $639 \times 572$  pixels,  $1440 \times 1080$  pixels, and  $257 \times 244$  pixels, respectively. Fig.5(b) shows the image after preprocessing and segmentation. Fig. 5(c) shows the image after removing point noise. Fig. 5(d) shows the image after removing block noise. Fig.5(e) shows the detection results of the linear structure,

and the detected linear structure is labeled with green. Fig. 5(f) is an image of crack texture skeleton feature analysis, that is, the skeleton feature of the image after removing the linear structure is extracted to identify the real crack, and the direction of the crack can be clearly observed through the skeleton diagram. Fig. 5(g) marks the cracks on the original images according to the final results of crack detection.

It can be seen that for the image with less background interference and clear crack contrast, the image crack area is obvious and the noise is less after preprocessing and block segmentation, which can quickly realize crack detection. For the images with more interference and unclear crack texture in the image background, more noise will be generated after block segmentation. The interference of noise can be effectively removed by analysis of connected domain features. For the images with linear structural features, probabilistic Hough transform can be used to detect them effectively. Finally, by use of the skeleton feature extraction algorithm, the interference of the pseudo crack texture can be eliminated, and thus the detection of the real crack is realized.

In this experiment, the zero-order moment threshold  $T_n$  was set to be 350, the rectangularity threshold  $T_r$  is set to be 0.3. The crack width was within 6 pixels, the width changed uniformly, and the ratio  $t_k$  of the number of pixels in the binary image to the number of pixels in the refined image did not exceed 6.

## 4.2 Crack image detection

Fig. 6 shows the detection results of five selected concrete surface cracks.

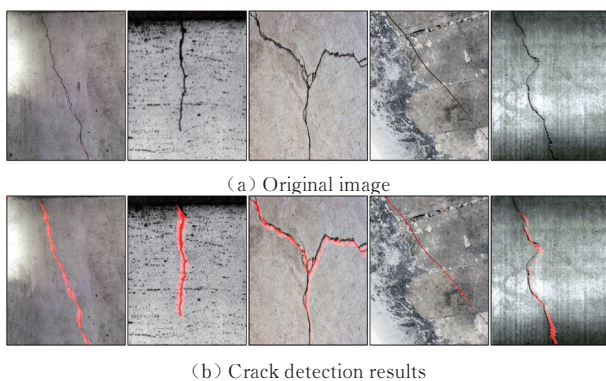


**Fig. 6** Detection results of common cracks

Fig. 6(a) is the original image with the sizes of  $1080 \times 1440$  pixels,  $377 \times 390$  pixels,  $400 \times 300$  pixels,  $505 \times 533$  pixels,  $237 \times 288$  pixels, respectively. There are few interference in the background of the image, and the crack area features are obvious. Fig. 6(b) shows the crack detection results. Since the gray level of the image crack

area changes greatly, there is a crack, but it does not affect the judgment of the overall trend of the crack.

Fig. 7 shows the detection results five selected subway tunnel surface cracks. Fig. 7(a) is the original image with sizes of  $420 \times 560$  pixels,  $385 \times 390$  pixels,  $626 \times 834$  pixels,  $200 \times 287$  pixels, and  $395 \times 516$  pixels, respectively. The image texture features are complex, and there are many interference objects in the image background. Fig. 7(b) shows the detection results of subway tunnel cracks, in which the crack contrast is clear and the noise is less. The crack part can be accurately detected by this algorithm. For the image with the gray level of crack close to the background, the local area of crack texture will break.

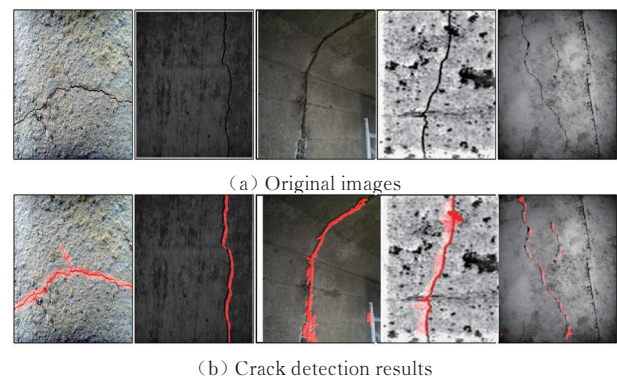


**Fig. 7** Detection results of surface cracks in subway tunnel

## 4.3 Evaluation indicators

To quantitatively analyze the effectiveness of the proposed method, the detection rate ( $R_D$ ) and the false detection rate ( $R_F$ ) were used as evaluation indicators, namely

$$R_D = \frac{p}{p+q}, \quad (14)$$

$$R_F = \frac{q}{p+q}, \quad (15)$$

where  $p$  is the number of correctly detected images, and  $q$  is the number of falsely detected images.

The results of detecting crack images with different scenes are shown in Table 1. The detection rate of common crack images can reach more than 90%, and the crack characteristics are obvious due to the few background interferences. However, there are many interference factors in the actual subway tunnel crack images, especially some old lines, mechanical scratches, water seepage, and low contrast often cause false detection. The 50 subway tunnel crack samples selected have a detection rate of 86%. In the follow-up research, it is necessary to strengthen the applicability of

different types of pseudo crack textures to reduce the false detection rate.

**Table 1 Experimental results of detecting crack images with different scenes**

Test target	Quantity	Correct detection rate/%	False detection rate/%
Normal crack image	50	92	16
Tunnel crack image	50	86	24
Integrated crack image	100	89	21

## 5 Conclusions

A crack detection method based on crack features in subway tunnel images was proposed and experimented. Firstly, the combination of Retinex smoothing and piecewise linear stretching was used to reduce the influence of uneven illumination and low contrast, and the initial segmentation of the image was realized by the Otsu threshold segmentation algorithm for block processing. Then, the interference of noise was filtered out by analyzing the image connected domain features, the influence of linear structural features on crack detection was removed by probabilistic Hough transform, and the pseudo crack interference was filtered out by image skeleton feature extraction algorithm. In this study, common crack images and actual crack images of subway tunnels were tested, and the detection rates of conventional crack images and tunnel crack images can reach 92% and 86%, respectively.

## Acknowledgement

This work was supported by National Natural Science Foundation of China (No. 61761027)

## Declaration of conflicting interests

The authors have no conflict of interests related to this publication.

## References

- [ 1 ] HE G H, LIU X G, CHEN Y Y, et al. Apparent tunnel diseases identification based on digital images. *Journal of Chongqing Jiaotong University (Natural Science Edition)*, 2019, 38(3): 21-26.
- [ 2 ] LUO J, LIU D G. Tunnel crack extraction based on adaptive threshold and connected domain. *Journal of Southwest Jiaotong University*, 2018, 53(6): 1137-1141.
- [ 3 ] WANG R, QI T Y. Study on crack characteristics based on machine vision detection. *China Civil Engineering Journal*, 2016, 49(7): 123-128.
- [ 4 ] TANG Q L, TAN Y, PENG L M, et al. On crack identification method for tunnel linings based on digital image technology. *Journal of Railway Science and Engineering*, 2019, 16(12): 3041-3049.
- [ 5 ] LI Q Q, ZOU Q, MAO Q Z. Pavement crack detection based on minimum cost path searching. *China Journal of Highway and Transport*, 2010, 23(6): 28-33.
- [ 6 ] WANG P R, HUANG H W, XUE Y D. Automatic recognition of cracks in tunnel lining based on characteristics of local grids in images. *Chinese Journal of Rock Mechanics and Engineering*, 2012, 31(5): 991-999.
- [ 7 ] WANG R, QI T Y, LEI B, et al. Characteristic extraction of cracks of tunnel lining. *Chinese Journal of Rock Mechanics and Engineering*, 2015, 34(6): 1211-1217.
- [ 8 ] XU G, ZHAO T Y, JIANG S, et al. Extraction method of structural surface cracks based on multiple connected domain features. *Journal Huazhong University of Science and Technology (Natural Science Edition)*, 2019, 47(10): 52-55.
- [ 9 ] OLIVEIRA H, CORREIA P L. Automatic road crack detection and characterization. *IEEE Transactions on Intelligent Transportation Systems*, 2013, 14(1): 155-168.
- [10] MEDINA R, LLAMAS J, GÓMEZ-GARCÍA-BERMEJO J, et al. Crack detection in concrete tunnels using a gabor filter invariant to rotation. *Sensors*, 2017, 17(7): 1-16.
- [11] SALARI E OUYANG D. An image-based pavement distress detection and classification//*IEEE 2012 International Conference on Electro Information Technology*, May 6-8, 2012, Washington, DC, USA. New York: IEEE Press, 2012: 1-6.
- [12] HE Y, FANG S. A local multi-scale Retinex algorithm for foggy image. *Journal of Hefei University of Technology*, 2015, 38(10): 1333-1338.
- [13] ZHANG Z H, YIN X Z, WANG Y P, et al. Research on image-based crack detection method for subway tunnel based on feature analysis. *Journal of Railway Science and Engineering*, 2019, 16(11): 2791-2800.
- [14] ZHU L Q, BAI B, WANG Y D, et al. Subway tunnel crack identification algorithm based on feature analysis. *Journal of the China Railway Society*, 2015, 37(5): 64-70.
- [15] SONG T, PANG S C, HAO S H, et al. A parallel image skeletonizing method using spiking neural p systems with weights. *Neural Processing Letters*, 2019, 50(2): 1485-1502.

## 基于多特征分析的地铁隧道裂缝检测

樊炜玮, 王小鹏\*, 朱生阳

兰州交通大学 电子与信息工程学院, 甘肃 兰州 730070

**摘要:** 在地铁隧道裂缝检测过程中, 由于隧道环境复杂及光照条件有限, 隧道裂缝检测比较困难。为此, 提出了一种基于多特征分析的隧道裂缝检测方法。首先, 利用Retinex匀光与分段线性拉伸相结合的预处理算法对图像进行增强处理, 通过分块处理的Otsu阈值分割算法实现图像的初步分割。其次, 对图像连通域面积和矩形度进行分析, 利用概率Hough变换提取图像中的线型结构特征, 利用连通域图像骨架特征提取算法滤除伪裂缝干扰, 最终实现真实裂缝检测。实验结果表明, 本方法对传统裂缝图像检测率可达92%, 对隧道裂缝图像检测率可达86%。实验结果证明了该方法的有效性。

**关键词:** 地铁隧道; 裂缝检测; 特征分析; 连通区域

**引用格式:** FAN Weiwei, WANG Xiaopeng, ZHU Shengyang. Crack detection in subway tunnels based on multi-feature analysis. *Journal of Measurement Science and Instrumentation*, 2024, 15(1): 140-147.